JOURNAL OF MATERIALS SCIENCE 25 (1990) 1699–1710

Microstructural development in non-oriented lamination steels

Part 2 *Isothermal transformation studies*

J.-W. LEE*, S. W. THOMPSON‡, P. R. HOWELL
Department of Materials Science and Engineering, The Pennsylvania State University, University Park, PA 16802, USA

The isothermal decomposition of austenite in two commercial low carbon (0.04 w/o) steels has been examined using scanning electron microscopy and transmission electron microscopy. Particular emphasis has been placed on analysing the pearlite reaction and the development of massive films of cementite at pro-eutectoid ferrite/pearlite interfaces. Similarly, grain boundary precipitation of cementite has been investigated. The results strongly support the contention that films of cementite at ferrite/pearlite interfaces form predominantly by a coarsening process. In addition, it is shown that grain boundary precipitation of cementite can occur from supersaturated ferrite or from the decomposition of austenite. Examination of the early stages of the pearlite reaction has provided evidence that multiple nucleation of cementite can be a necessary precursor to the development of a pearlite colony.

1. Introduction

In a previous report, two of the present authors documented the nature of the ferrite/pearlite aggregates in two low carbon steels [1]. In [1], some limited evidence for the operation of Hillert's branching mechanism [2] was presented. In addition, some of the experimental data suggested that multiple nucleation of cementite, at the pro-eutectoid ferrite/austenite interface, was the formative step in the nucleation of a pearlite colony. In order to document more fully the initiation of the pearlite reaction, a series of isothermal transformation studies have been performed. This has permitted the early stages of the pearlite reaction to be documented.

Lee and Howell [1] also observed that massive films of cementite were located at ferrite grain boundaries and at ferrite/pearlite interfaces. In [1], three possibilities for cementite film formation were proposed:

(1) the massive films at ferrite grain boundaries formed directly from austenite with a high aspect ratio;

(2) the massive films at pearlite/ferrite interfaces were due to nucleation and growth of cementite on the pro-eutectoid ferrite/austenite interfaces, prior to impingement with a pearlite colony; and

(3) the films at pearlite/ferrite interfaces developed by a coarsening process at the impingement interface of pearlite with pro-eutectoid ferrite, via diffusion of carbon from supersaturated ferrite.

However, these studies were conducted on continuously cooled specimen material and substantial coarsening of the cementite films occurred during cooling. Hence, a further objective of the isothermal transformation study is to examine the development of massive cementite films, both as a function of transformation time and transformation temperature.

2. Experimental details

Two low carbon steels in the form of hot rolled strips were obtained from Inland Steel. The compositions of these steels is given in Table I.

Specimen materials were austenitized at 1000° C for 5 min, isothermally transformed in a salt bath and quenched in iced water. Table II gives the temperatures and times employed in the present study for the isothermal transformation. This schedule was devised so that the initiation of the pearlite reaction could be studied (e.g. in the range from 10 to 1.8×10^2 sec at 700° C). Similarly the morphology of the untransformed austenite could be related to the morphology of both the pearlite and the intergranular cementite. In addition, much longer transformation times were employed (e.g. 5.4×10^4 sec at 700° C) to investigate the effect of extended annealing treatments on the nature of the product phases.

Specimens for scanning electron microscopy (SEM) were prepared using standard metallographic techniques, etched in 2% nitric acid in methanol and examined in an ISI Super IIIA operating at 25 kV. Specimens for transmission electron microscopy (TEM) were prepared in a twin-jet electro-polisher using an electrolyte consisting of 5% perchloric acid in

Present address: Department of Metallurgical Engineering and Materials Science, Carnegie-Mellon University, PA 15213, USA.
‡*Present address*: Advanced Steel Processing and Products Research Center, Department of Metallurgical and Materials Engineering, Colorado School of Mines, CO 80401, USA.

0022–2461/90 $03.00 + .12

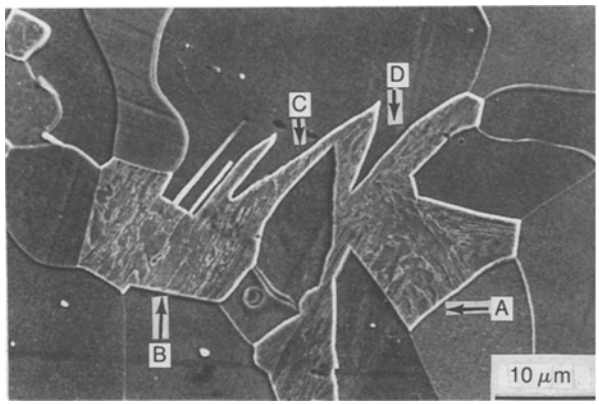

Figure 1 The ferrite/austenite microstructure developed after 10 sec at 650° C (steel A).

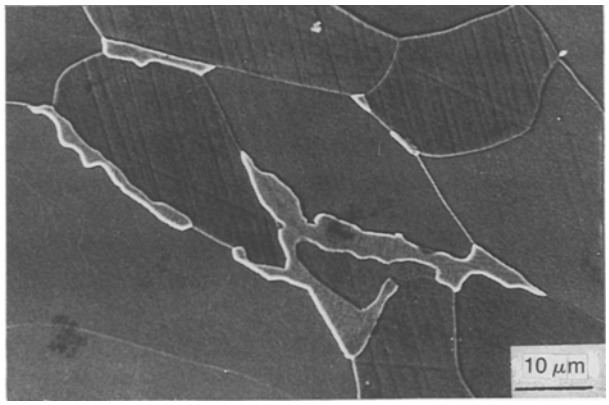

Figure 2 Ferrite and austenite in steel A after 60 sec at 550° C.

glacial acetic acid at room temperature and at a potential of 35 V. TEM was performed using a Philips EM 300 operating at 100 kV.

3. Results

In view of the large number of specimens which were investigated (Table II), Section 3.1 presents some results which are typical for all transformation temperatures employed. Sections 3.2 and 3.3 document, in some detail, the progress of austenite decomposition as a function of time at 700 and 675° C. Section 3.4 is concerned with the isothermal reactions which occur at lower temperatures. In this section, the results presented are selective and are included to illustrate certain phenomena (e.g. the initiation of the pearlite reaction). The relevance of these observations is discussed in Section 4.

3.1. General

At all temperatures investigated, the initiation of the ferrite reaction was extremely rapid. Fig. 1 is a typical micrograph of the ferrite/austenite* microstructure developed in steel A after 10 sec at 650° C. It is interesting to note that many of the ferrite/austenite interfaces are accurately planar (e.g. at A and B) and certain ferrite grains are developing Widmanstatten side plates (e.g. at C and D). At lower transformation temperatures, austenite with a high aspect ratio was often observed as shown in Fig. 2.

The kinetics of the pearlite reaction were highly erratic. This may be gauged from Fig. 3 which is from specimen material which had been transformed at 675° C for 1.8×10^2 sec. As can be seen, the transformation of austenite to pearlite is complete at A, whereas the pearlite reaction has not been initiated within the other pools of austenite. It is also interesting to note that the majority of the untransformed pools of austenite are surrounded by three or more ferrite grains. Due to the erratic nature of the pearlite reaction, it is difficult to quote precise results concerning initiation and completion times, although these times decreased with decreasing transformation temperature. For example, the pearlite reaction in steel A was completed after 3.6×10^3 sec at 700° C whereas only approximately 3×10^2 sec was required at 550° C.

Figs 4 to 7 are typical bright field TEM images of both fully and partially transformed specimen materials. Small islands of retained austenite were often observed and Fig. 4 shows a typical example of a retained austenite particle. Large pools of austenite transformed to martensite during quenching and the martensite exhibited a plate-like morphology as shown in Fig. 5. The ferritic matrix was found to contain a high number density of small plate-like features together with sub-boundaries (see Fig. 6). To date, it is uncertain whether the small plate-like features are carbide precipitates or vacancy loops. The pearlitic ferrite contained a relatively low dislocation density (Fig. 7) and the pearlitic cementite frequently coarsened at the impingement interface between the colony and the abutting pro-eutectoid ferrite. This latter observation will be discussed in subsequent sections.

TABLE I Chemical composition of specimen materials (in wt %)

	C	Mn	Si	P	S	Al
Steel A	0.04	0.6	0.05	0.06	0.02	< 0.008
Steel B	0.04	0.7	0.22	0.09	0.02	0.21

TABLE II Isothermal transformation schedule

Temperature (° C)	Times (sec)
700	10, 30, 1.8×10^2, 6×10^2, 3.6×10^3, 1.8×10^4, 5.4×10^4
675	30, 1.8×10^2, 3.6×10^3, 1.8×10^4, 5.4×10^4
650	10, 60, 3×10^2, 1.8×10^3, 3.6×10^3, 1.8×10^4
625	60, 3×10^2, 1.8×10^3, 3.6×10^3
600	60, 3×10^2, 1.8×10^3, 3.6×10^3
575	60, 3×10^2, 1.8×10^3, 3.6×10^3
550	60, 3×10^2, 1.8×10^3, 3.6×10^3

*It should be appreciated that the majority of the austenite transforms to martensite during the quench. However, the term austenite will be employed since the major emphasis of this investigation is the high temperature decomposition of austenite.

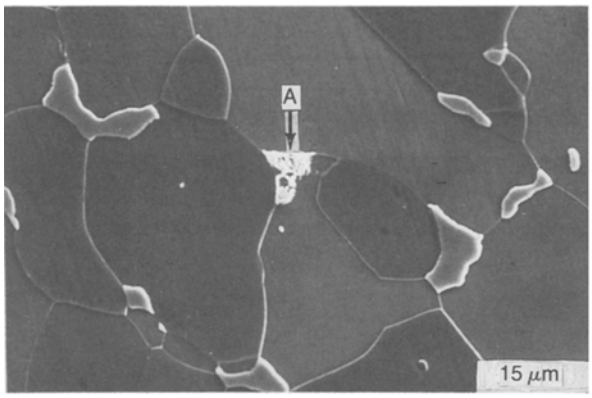

Figure 3 Ferrite, pearlite and austenite after 1.8×10^2 sec at 675° C (steel A).

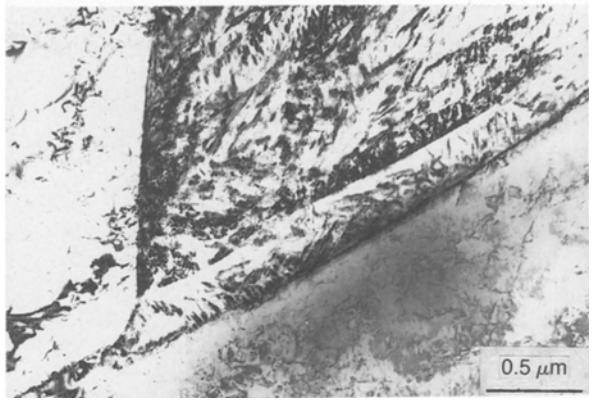

Figure 5 Martensite in steel B (60 sec at 575° C).

3.2. Isothermal transformation characteristics at 700° C

After 180 sec at 700° C, the pearlite reaction had not commenced in either steel. The ferrite/austenite microstructures were very similar to those shown in Figs 1 and 2, i.e., faceted α/γ interfaces and austenite of a high aspect ratio. However, no evidence for the formation of Widmanstatten side plates was found at this temperature.

Fig. 8 shows steel B which had been transformed at 700° C for 6×10^2 sec. The microstructure consists predominantly of pro-eutectoid ferrite and austenite. However, some discrete cementite precipitates are located at the ferrite grain boundaries (arrowed). At a higher magnification (from a different region of the specimen), Fig. 9 clearly shows the presence of cementite precipitates on ferrite grain boundaries. The variability of the kinetics of the pearlite reaction may be gauged by comparing Fig. 10 with Fig. 8. In Fig. 10, the pearlite reaction is complete (compare with Fig. 8 where *no* pearlite has developed), and evidence is observed at A for the partial formation of a continuous film of cementite on the pro-eutectoid ferrite/pearlite interface. It should also be noted that the pearlitic cementite is lamellar in nature. The active nucleus [2] for this pearlite colony is grain 1 since no boundary is observed between the pro-eutectoid ferrite grain 1 and the pearlitic ferrite.

After 3.6×10^3 sec at 700° C, some residual islands of austenite still remain although the pearlite reaction is complete in most regions of the specimen. An example of a pearlite colony is given in Fig. 11. Massive films of cementite are located at the periphery of the colony at A and B, whilst at C, extensive coarsening of the cementite at the ferrite/pearlite interface is observed and individual cementite lamellae exhibit a "club-like" morphology at the pearlite/ferrite interface. Fig. 12 is an example of the precipitation of cementite on ferrite grain boundaries. The precipitates are discrete in nature and have caused considerable puckering of the boundary. Massive films of cementite on ferrite grain boundaries were also observed for this ageing time.

After 1.8×10^4 sec at 700° C, the pearlite reaction is complete, and the massive films of cementite on the ferrite/pearlite interfaces have thickened appreciably (Fig. 13). Similarly, massive films of cementite are present on the ferrite grain boundaries (Fig. 14). An example of a fully transformed region in steel B is shown in Fig. 15. Note the non-lamellar nature of the pearlitic cementite and the massive film of cementite on the interface between ferrite grain 1 and the pearlitic colony. Finally, Fig. 16 is an example of the puckering of a ferrite grain boundary by small discrete cementite precipitates.

3.3. Isothermal transformation characteristics at 675° C

In essence, the sequence of events of 675° C was similar to that at 700° C. Figs 17 and 18 show examples of the initiation of the pearlite reaction in steel A after 30 sec.

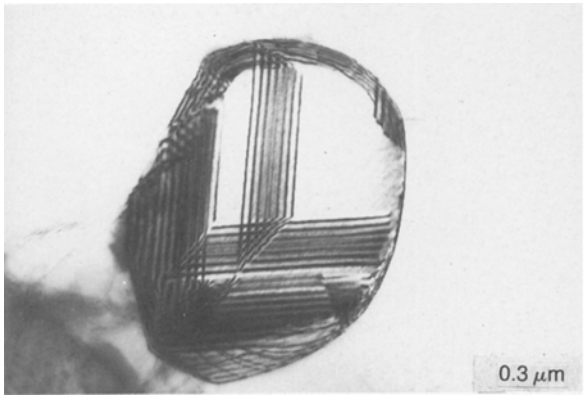

Figure 4 A retained austenite particle (steel B, after 3×10^2 sec at 625° C).

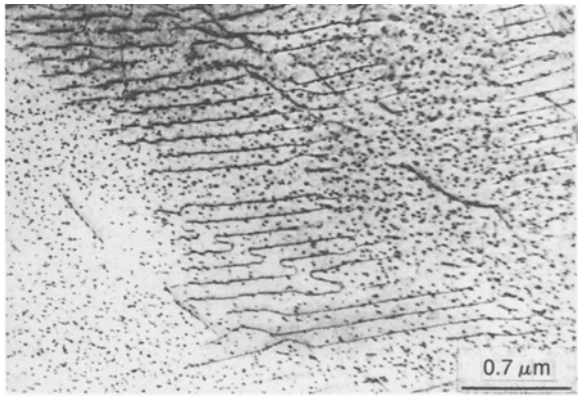

Figure 6 The ferrite microstructure in steel B (after 3×10^2 sec at 625° C).

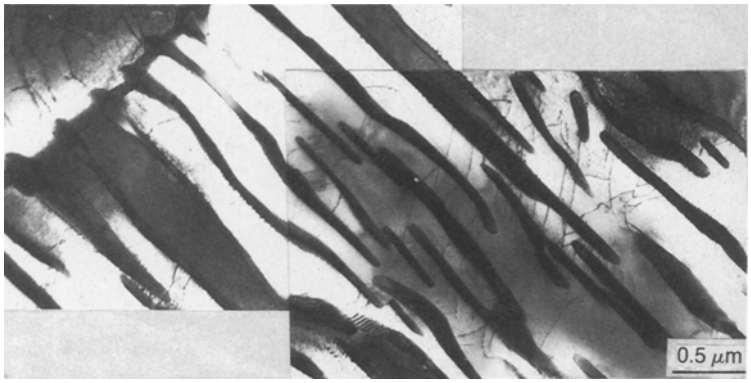

Figure 7 TEM image of a pearlite colony in steel B (after 3×10^2 sec at 550° C).

In all these figures, ferrite grain 1 is the active nucleus for the pearlite colonies which are consuming the austenite (A). Figs 17a and b illustrate an "inverse branching" effect where two cementite lamellae coalesce to form one lamellae (arrowed). These observations are of interest in that the classic branching mechanism [2] involves the formation of two, or more, cementite lamellae from one. Fig. 18 shows a complex, faceted pearlite/austenite interface. It is likely that for Figs 17 and 18 the initiation site for the pearlite reaction is very close to the plane of polish. This indicates that multiple nucleation of cementite has occurred on the pro-eutectoid ferrite/pearlite interface prior to the development of the pearlite colony. It is also interesting to note that there are more cementite "lamellae" at the pearlite initiation site than at the position of the pearlite/austenite interface. For example, in Fig. 17a the number of cementite lamellae is reduced from 14 to 11, while in Fig. 18, the number is reduced from *ca.* 50 to *ca.* 30. Further discussion of these figures is deferred to Section 4.5.

Figs 19 and 20 are from specimen material which had been transformed at 675° C for 1.8×10^2 sec. Fig. 19 (steel A) shows approximately lamellar pearlite together with regions of untransformed austenite (A). Again, the faceted nature of the ferrite/austenite interfaces should be noted. At this stage, there is little evidence for the formation of massive films of cementite on the ferrite/pearlite interfaces. Fig. 20 is from steel B and the pearlite colonies are non-lamellar. In common with Fig. 19, many of the γ/α interfaces are faceted. Grain boundary precipitation of cementite is also observed in Fig. 20 (arrowed).

After 3.6×10^2 sec, the pearlite reaction is complete in both steels. Fig. 21 is an example of pearlitic colonies and illustrates the formation of massive films of cementite at ferrite/pearlite interfaces and at ferrite grain boundaries.

Continued ageing leads to an increase in the thickness of the cementite films as illustrated in Fig. 22.

3.4. Isothermal transformation characteristics at low temperatures (650° to 550° C)

The transformation characteristics at low temperatures were similar to those documented at 700 and 675° C. Fig. 23 shows a series of pearlite colonies in steel B which had been transformed at 650° C for 3.6×10^3 sec. In this figure, both lamellar and non-lamellar pearlite colonies are present. It is interesting to note that the tendency towards the formation of non-lamellar pearlite is not appreciably greater at low temperatures than at 675° or 700° C. However, the films of cementite are less well developed. This latter point is amplified in Figs 24 and 25 where the grain boundary cementite in steels A and B, respectively, is discrete in nature. However, after extended transformation times, massive films of cementite were observed.

Figs 26 and 27 show specimen material which had been transformed at 600° C for 1.8×10^3 sec and 3.6×10^3 sec, respectively. Fig. 26 (steel A) shows an approximately lamellar pearlite nodule together with massive films of cementite at both ferrite grain boundaries and pearlite/ferrite interfaces. The partial cementite film at point A still exhibits some "club-like" characteristics and it is likely that this film is forming by a coarsening process. Fig. 27 (steel B), shows a

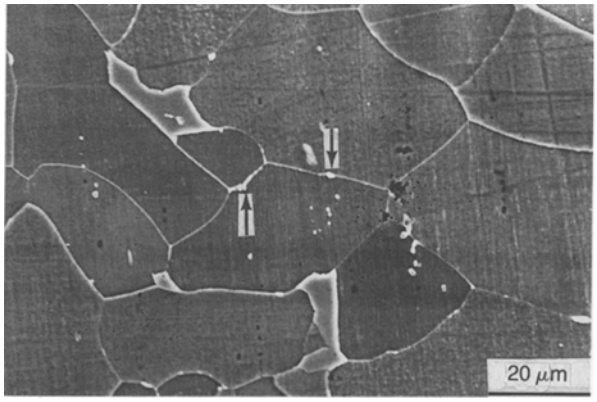

Figure 8 Precipitation of cementite on ferrite grain boundaries (steel B after 6×10^2 sec at 700° C).

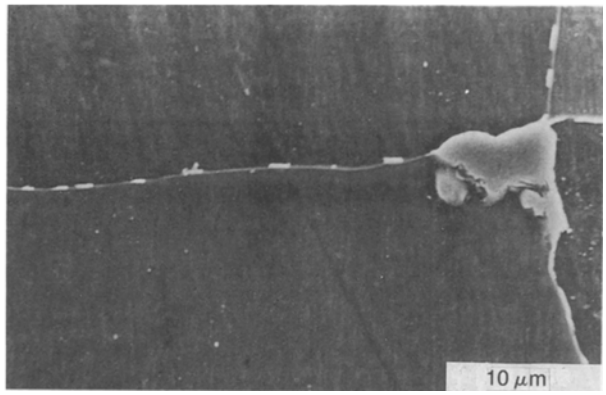

Figure 9 Discrete precipitates of cementite on ferrite grain boundaries (steel B after 3×10^2 sec at 700° C).

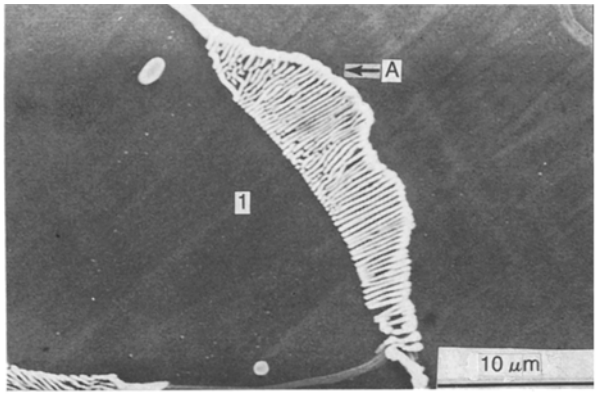

Figure 10 Pearlite in steel B (after 6×10^2 sec at 700° C).

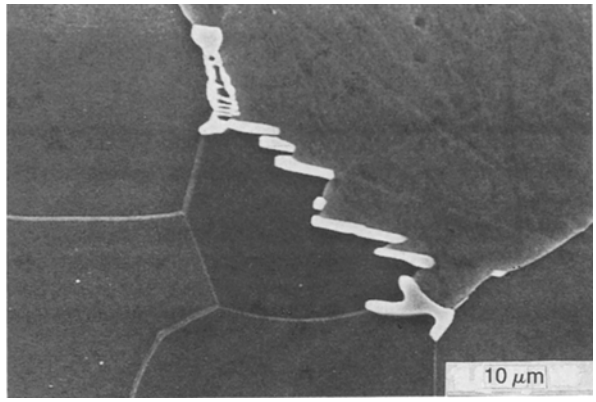

Figure 12 Pearlite and grain boundary cementite (steel A after 3.6×10^3 sec at 700° C).

non-lamellar pearlite colony together with massive films of cementite at several grain boundaries. The thickness of the films are less than those developed after equivalent transformation times at the higher temperatures of 700°, 675° and 650° C.

Figs 28 and 29 are micrographs of steel B which had been isothermally transformed at 575° C for, 1.8×10^3 and 3.6×10^3 sec, respectively. Fig. 28 illustrates an embryonic pearlite colony (A) together with a grain boundary which has been puckered by precipitation of cementite (B). It is interesting to note the lamellae in the embryonic colony are parallel to the "discrete" precipitates on the adjacent ferrite grain boundary. The relevance of this is discussed in Section 4.2. Coarsening of cementite at the ferrite/pearlite interface is beginning to occur after 3.6×10^3 sec as shown in Fig. 29.

Figs 30 and 31 are bright field TEM micrographs of specimen material after 60 sec at 550° C (steel A). In both instances, pro-eutectoid ferrite grain 1 is continuous with the pearlitic ferrite which is further evidence that pro-eutectoid ferrite is the active nucleus for pearlite. It should be noted that the impingement interface between pearlite and ferrite (arrowed in Fig. 30) is associated with coarsened cementite which displays a "club-like" morphology. It is also interesting to note that individual "clubs" are beginning to coalesce. In Fig. 31 the pearlite is associated with untransformed austenite (A). The development of this colony appears to occur in a manner which is very similar to that described by Fournelle and Clarke [3]

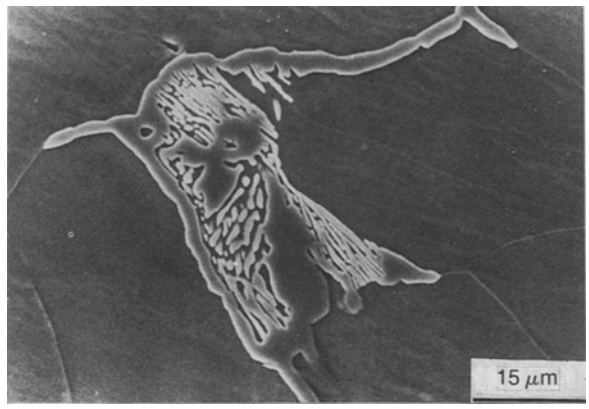

Figure 13 Massive cementite films in association with both pearlite colonies and ferrite grain boundaries (steel A after 1.8×10^4 sec at 700° C).

(see Figs 9 and 11 of their paper) for the discontinuous reaction in Cu–In alloys. This particular mechanism involves the formation of multiple "U-shaped" allotriomorphs at the initiation interface.

Finally, Fig. 32 shows pearlite colonies of high aspect ratio together with thin films of cementite at grain boundaries (arrowed). The propensity towards the formation of pearlite with high aspect ratio is striking at these low temperatures and the cementite films are less well developed compared with transformations at higher temperatures.

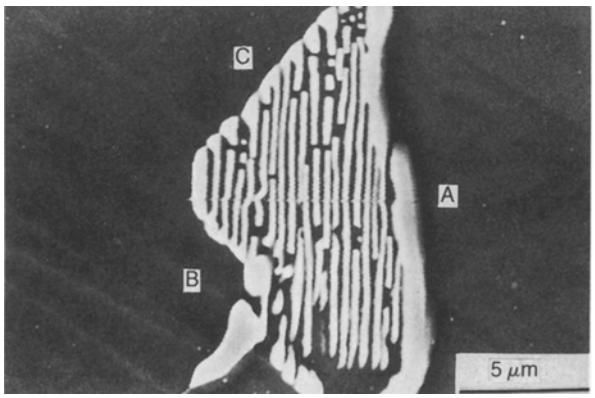

Figure 11 Pearlite and massive films of cementite (steel A after 3.6×10^3 sec at 700° C).

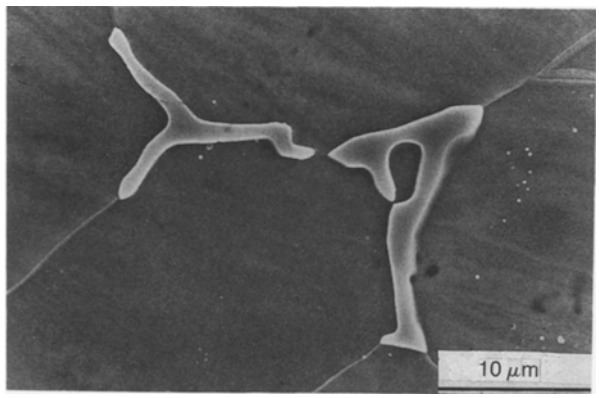

Figure 14 Cementite at ferrite triple junctions (steel A after 1.8×10^4 sec at 700° C).

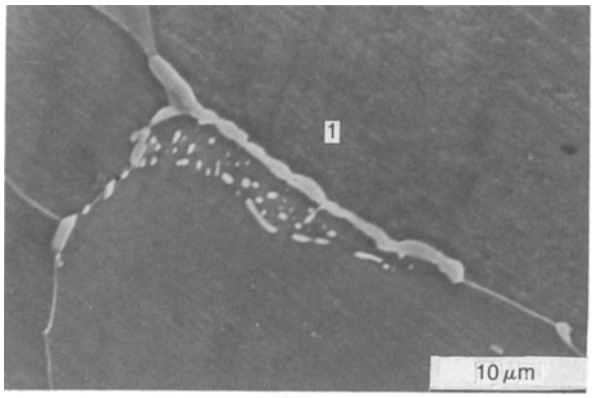

Figure 15 Non-lamellar pearlite together with a massive film of cementite (steel B after 1.8×10^4 sec at 700° C).

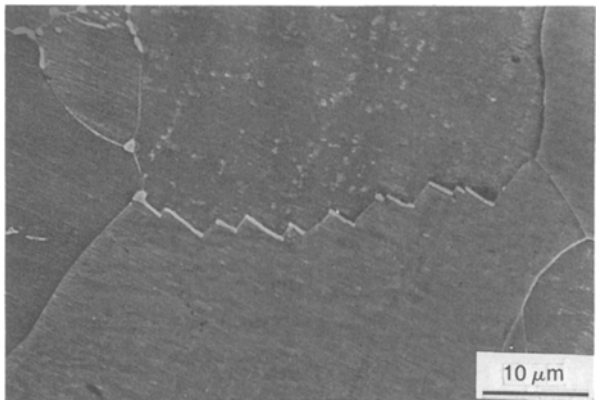

Figure 16 Grain boundary puckering by discrete cementite precipitates (steel B after 1.8×10^4 sec at 700° C).

3.5. The effect of transformation temperatures on the size and morphology of pearlite, austenite and films of cementite

Figs 33 and 34 plot the average aspect ratios of austenite and pearlite, and the average size of the austenite and pearlite, respectively, as a function of transformation temperature. The aspect ratio of the austenite increases almost linearly with decreasing transformation temperature as does the aspect ratio of the pearlite (see Fig. 33). Similarly, the size of both the austenite and pearlite decreases slightly with decreasing transformation temperature (see Fig. 34).

Fig. 35 plots the cementite film thickness for transformation temperatures of 650° C and above as a function of time. As can be seen

(1) the film thickness increases with time up to *ca.* 5 h, after which little increase in film thickness is observed; and

(2) for a given isothermal transformation time, the film thickness increases with increasing transformation temperature.

For temperatures below 650° C, the variation of film thickness with time was similar to that at 650° C.

4. Discussion

The isothermal decomposition of austenite in the steels investigated exhibited complex characteristics. In the following sub-sections, the major features of the transformation of austenite to ferrite/carbide aggregates are discussed. In Section 4.1, the effects of isothermal transformation temperature on the microstructure are discussed. Sections 4.2 to 4.5 discuss specific phenomena including:

(1) the development of massive films at ferrite grain boundaries (Section 4.2.);

(2) the origin of discrete precipitates on ferrite grain boundaries (Section 4.3);

(3) the formation of massive films at ferrite/pearlite interfaces (Section 4.4); and

(4) the pearlite reaction (Section 4.5).

4.1. The effect of transformation temperature on the decomposition products

Changing the transformation temperature from 700° to 550° C led to a change in the scale of the microstructure. However, the nature of the transformation products remained essentially unchanged. For example, the dominant ferrite morphology was equiaxed over the entire temperature range and the propensity for the formation of non-lamellar pearlite did not appear to change with changing transformation temperature. However, cementite film formation at both ferrite/ferrite grain boundaries and ferrite/pearlite interfaces was more prevalent at the higher transformation temperatures. Since the formation of films at grain boundaries must be a competitor to pearlite formation, the above implies that film formation is a more favoured mode of austenite decomposition at higher transformation temperatures. Further discussion on this point is deferred to Sections 4.4 and 4.5.

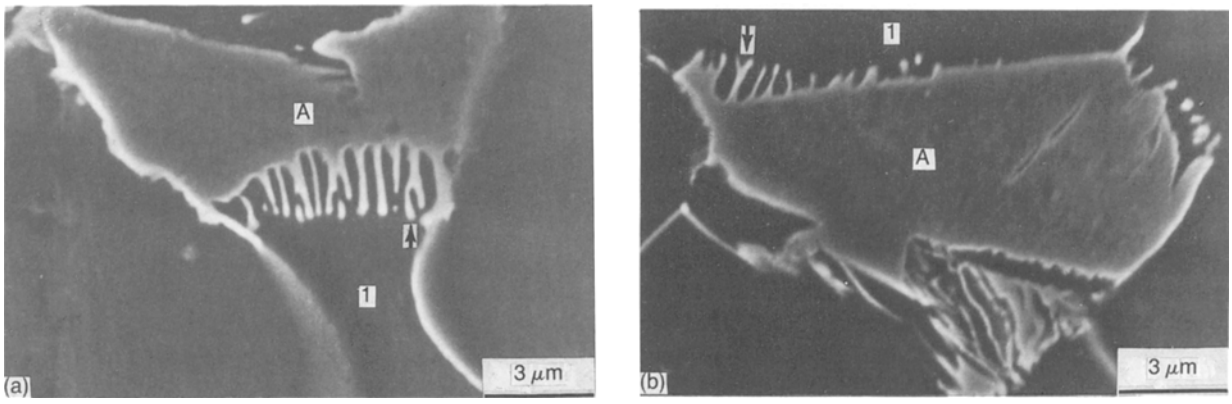

Figure 17 Inverse branching in steel A (30 sec at 675° C). In both instances, ferrite grain 1 is the active nucleus for the pearlite reaction.

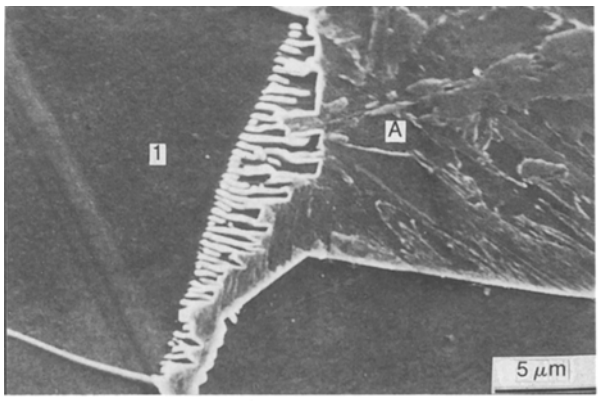

Figure 18 A partially transformed pool of austenite (steel A after 30 sec at 675° C).

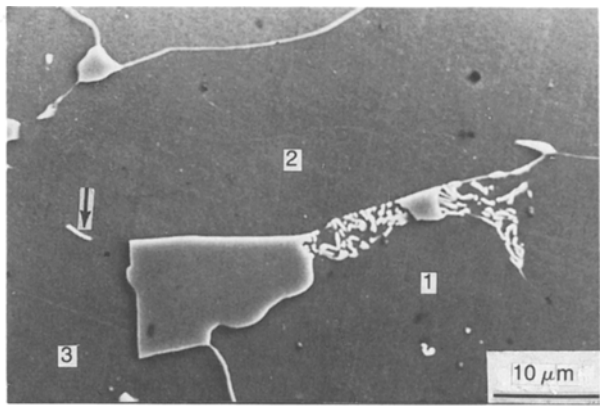

Figure 20 Ferrite, non-lamellar pearlite and austenite in steel B (after 1.8×10^2 sec at 675° C).

The data presented in Fig. 33 show that both the aspect ratio of the austenite and that of the resultant pearlite increased with decreasing transformation temperature, while Fig. 34 indicated a decrease in size for both austenite and pearlite with a decrease in transformation temperature. These trends can be explained in terms of the ferrite reaction. As the temperature is reduced, the driving force for the proeutectoid ferrite reaction will be increased, the nucleation rate will increase and the average ferrite grain size will decrease. Hence, the entrapped pools of austenite (which subsequently transform to pearlite) will become smaller and less equiaxed as the transformation temperature is decreased. It is also interesting to note that the average aspect ratio of the austenite (Fig. 33a) is always greater than the aspect ratio of the pearlite (Fig. 33b) at a given transformation temperature. In addition, the average size of the pearlite is always greater than the average size of the austenite from which it is formed (see Fig. 34). These apparent discrepancies can be explained in terms of the fact that the austenite can transform to either pearlite or massive boundary films of cementite (see Section 4.2).

4.2. The formation of massive films of cementite at ferrite grain boundaries

Massive films of cementite at ferrite grain boundaries were a common occurrence (see Figs 13, 21, 22 and 26). It is most likely that these films form from austenite of a high aspect ratio (as seen in Fig. 2). A possible sequence of events is:

(1) precipitates of cementite form on one of the ferrite/austenite interfaces and coarsen by depleting the austenite in carbon;

(2) the carbon depleted austenite then transforms to ferrite leading to a continuous film of cementite at a ferrite grain boundary.

This sequence of events is shown in Fig. 25 of Lee and Howell [1].

In addition, the massive films of cementite were often associated with ferrite triple junctions (see Figs 12 and 14). Fig. 36 shows how these films can develop; the argument is essentially the same as that outlined for film formation at grain boundary faces. Hence, as suggested in Section 4.1, the formation of massive cementite films is a competitor to the pearlite reaction. This competitive reaction can also be used to explain the variation in both aspect ratio and size between the pearlite and the austenite (see Figs 33 and 34, and Section 4.1). Since it has been suggested that massive films of cementite form from austenite pools that are both small and of high aspect ratio, the pearlite will form from austenitic regions that are both of a higher average size and a lower average aspect ratio.

The increase in film thickness with ageing time (shown in Fig. 35) can be achieved in two ways:

(1) by the acquisition of carbon from supersaturated ferrite during isothermal annealing (see Section 4.3); and

(2) by conventional Ostwald ripening.

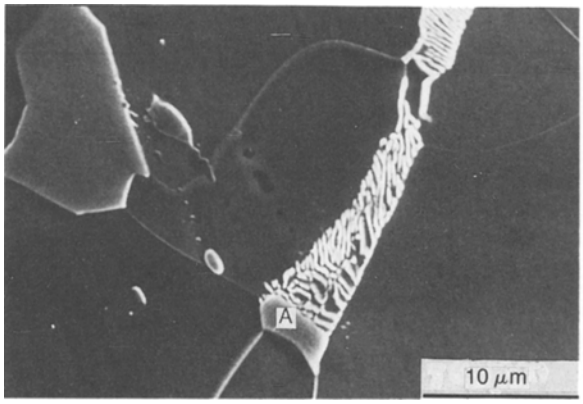

Figure 19 Ferrite, pearlite and austenite in steel A (after 1.8×10^2 sec at 675° C).

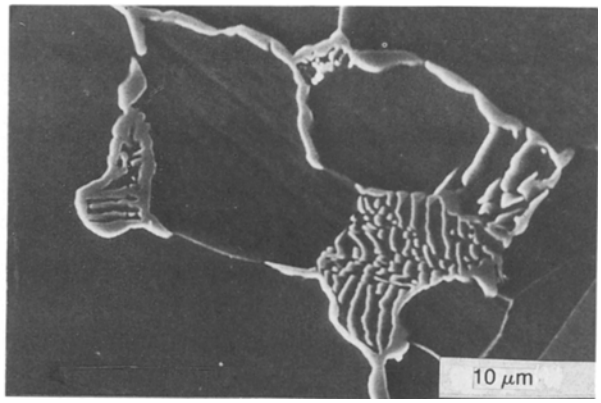

Figure 21 Pearlite and massive films of cementite (steel A after 3.6×10^2 sec at 675° C).

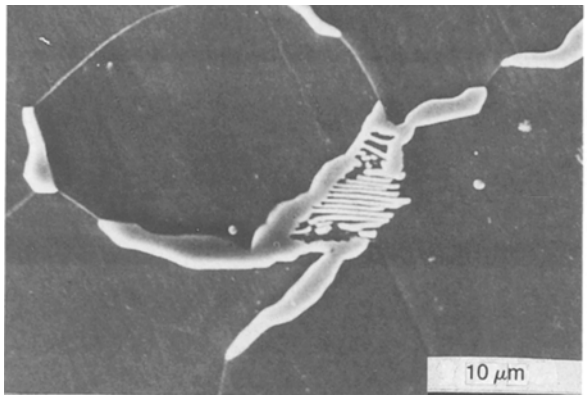

Figure 22 Pearlite and films of cementite (steel A after 1.8×10^4 sec at 675° C).

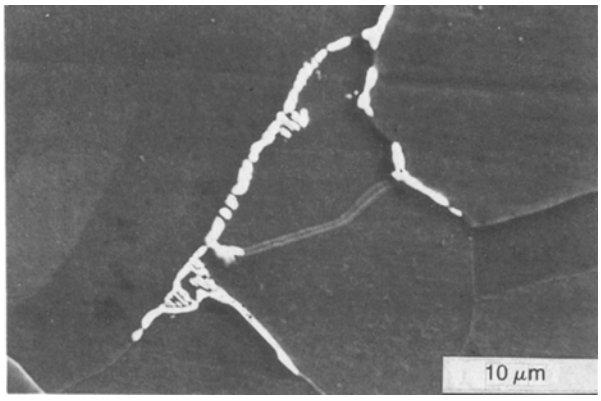

Figure 24 An embryonic pearlite colony (steel A after 3.6×10^3 sec at 650° C).

It is likely that step (1) contributes in the early stages but that Ostwald ripening will dominate after extended holding times at the transformation temperature.

In certain instances, it is difficult to differentiate between an ill-formed grain boundary film and an embryonic pearlite colony. For example, the distribution of cementite in Fig. 24 suggests that this corresponds to an embryonic pearlite colony. However, no definite conclusion can be drawn. A clearer example of a pearlite colony which has formed from austenite of high aspect ratio is shown in Fig. 28 where individual cementite lamellae are resolved at A. However, at B, a series of "discrete" precipitates are present. In view of the fact that these latter particles are of a similar width to those within the embryonic colony and their habit planes are virtually identical, it is suggested that the "grain boundary" precipitates at B formed at the interface between proeutectoid ferrite grain C and austenite of a high aspect ratio. The implications of this are:

(i) when the cementite plates form at a large angle to the pro-eutectoid ferrite/austenite interface, the pearlite reaction is favoured even for small transforming volumes;

(ii) when the cementite plates form at a shallow angle to the advancing interface, cooperation between the ferrite and cementite is more difficult to establish. Hence, the carbides grow by depleting austenite in carbon which then transforms to ferrite.

A similar situation is seen in Fig. 12, where the "discrete" precipitates and the lamellae within the small pearlite colony have almost identical habit planes and very similar widths.

As mentioned in Section 4.1, the propensity for film formation decreased with decreasing transformation temperature. Smaller austenite pools with higher aspect ratios transformed to pearlite when compared with the higher transformation temperatures. This is particularly evident in Fig. 32 where a number of pearlite colonies of very high aspect ratio are observed. Although no firm conclusion can be drawn, it is likely that the increased driving force for pearlite formation at the lower transformation temperatures will favour the development of cooperation between the phases, i.e. the establishment of a pearlite colony.

4.3. Precipitation from supersaturated ferrite

Small discrete precipitates of cementite were observed on ferrite grain boundaries (see Figs 8 and 9) and this discrete precipitation could lead to grain boundary puckering (see Fig. 16). Since these precipitates can form prior to the pearlite reaction (Figs 8 and 9) it is most likely that these precipitates form from supersaturated ferrite. In addition, they are often located in regions well removed from any pearlite colonies (Fig. 16). However, this explanation requires that the pro-eutectoid ferrite is supersaturated with respect to carbon. Supersaturation of the pro-eutectoid ferrite

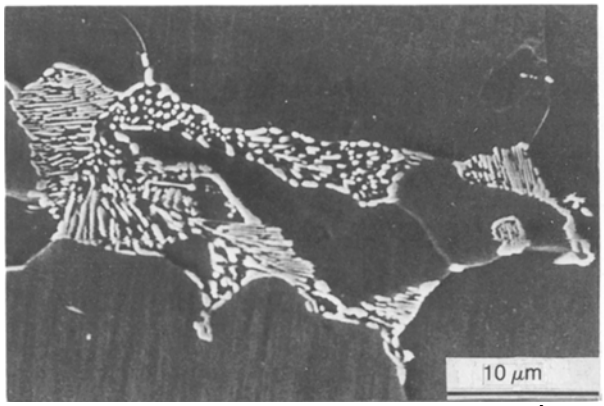

Figure 23 A series of pearlite colonies (steel B after 3.6×10^3 sec at 650° C).

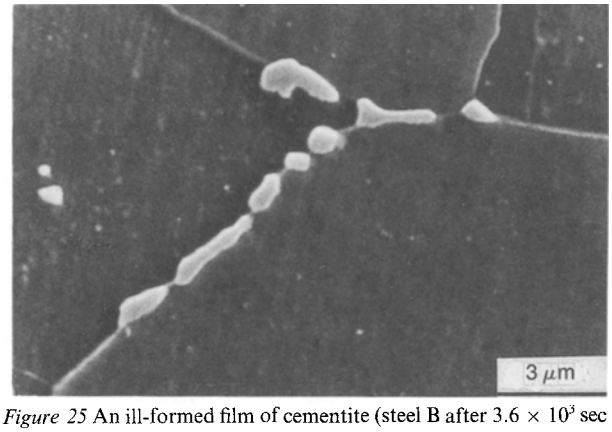

Figure 25 An ill-formed film of cementite (steel B after 3.6×10^3 sec at 650° C).

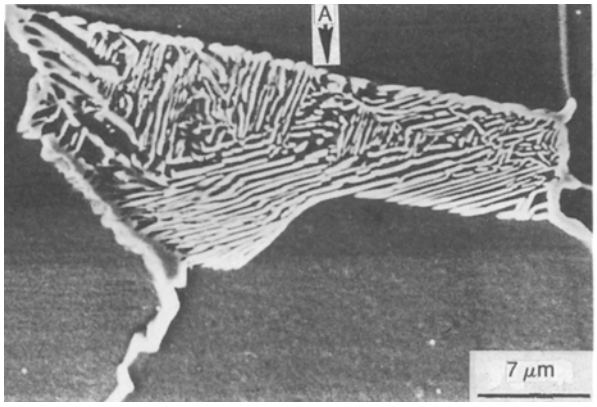

Figure 26 Lamellar pearlite in steel A (after 1.8×10^3 sec at 600° C).

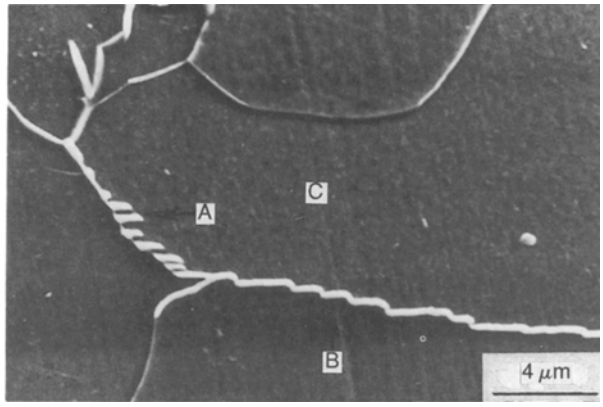

Figure 28 An embryonic pearlite colony together with grain boundary precipitation of cementite (steel B after 1.8×10^3 sec at 575° C).

may be explained by the following hypothesis. Consider Fig. 37 which is a schematic drawing of the Fe-rich end of the Fe–C phase diagram. If an alloy of composition C_0 is isothermally transformed at T_1, then at time $t = 0$, metastable equilibrium will exist between ferrite of composition $C\alpha_1$ and austenite of composition $C\gamma_1$ (these values are given by extrapolating the $\alpha/(\gamma + \alpha)$ and $\gamma/(\gamma + Fe_3C)$ solvus lines, respectively). However, the equilibrium carbon concentration in ferrite at T_1 is $C\alpha$. Hence, the pro-eutectoid ferrite will be supersaturated, the supersaturation being $(C\alpha_1 - C\alpha)$. This will lead to a driving force for precipitation of cementite, both within the matrix and on ferrite grain boundaries.

It should be noted that grain boundary puckering by multiple grain boundary precipitates has been suggested to be the formative step in the creation of certain discontinuous reactions [4]. Although a discontinuous reaction has not been observed in these steels, and is also highly unlikely due to the low carbon supersaturation, puckering has relevance to pearlite initiation as discussed in Section 4.5.

Finally, it is worth noting that the observation of puckering is not unambiguous evidence for the precipitation of cementite from ferrite. For example, in Figs 12 and 28 the boundaries are puckered. However, as discussed in Section 4.2, it is most likely that these precipitates formed on the austenite/ferrite interface. Hence, for these latter precipitates, grain boundary puckering occurs *after* the formation of cementite. Conversely, nucleation and puckering are concomitant

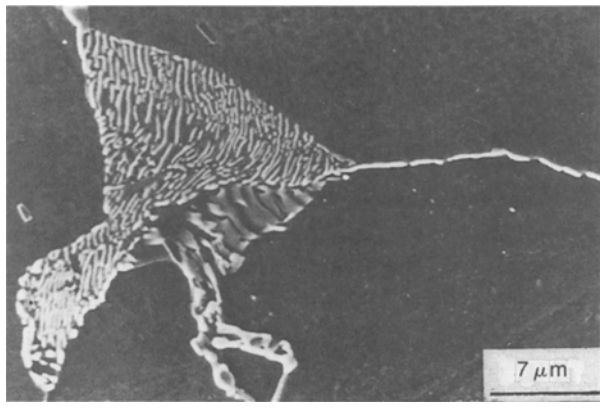

Figure 29 The onset of coarsening at pearlite/ferrite interfaces (steel B after 3.6×10^3 sec at 575° C).

processes when cementite forms on the ferrite grain boundaries.

4.4. The formation of massive films at ferrite/pearlite interfaces

As stated in Section 1, two possibilities for the formation of massive films at ferrite/pearlite interfaces were proposed by Lee and Howell [1]. These possibilities are:

(1) the massive films are due to the nucleation and growth of cementite on the pro-eutectoid ferrite/austenite interface prior to impingement with a pearlite colony; and

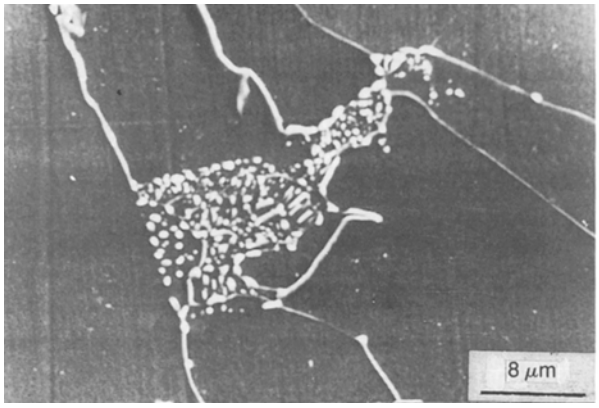

Figure 27 Non-lamellar pearlite in steel B (after 3.6×10^3 sec at 600° C).

Figure 30 Coarsening of cementite at a ferrite/pearlite interface (steel A after 60 sec at 550° C).

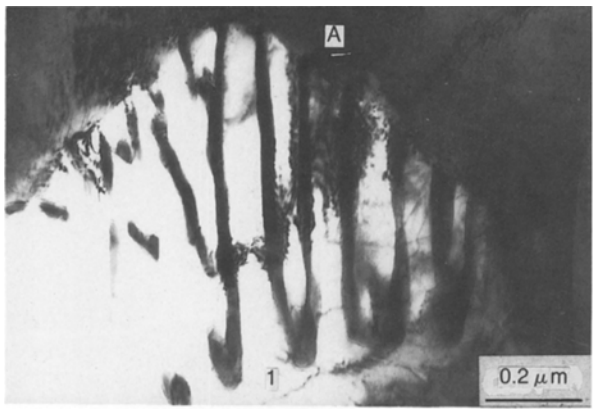

Figure 31 TEM image of a pearlite colony (steel A after 60 sec at 550° C).

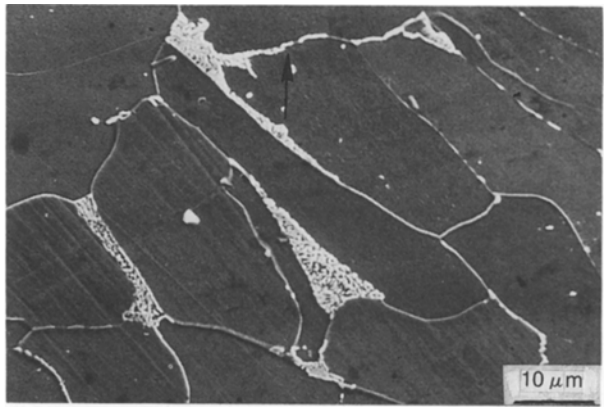

Figure 32 Elongated pearlite colonies in steel B (after 3.6×10^3 sec at 550° C).

(2) the films develop by a coarsening process at the pearlite/pro-eutectoid ferrite interface.

The results of the present investigation suggest strongly that the films form predominantly by a coarsening reaction. The reasons for this are as follows:

In the early stage of ageing, little evidence for *massive* film formation at ferrite/pearlite interfaces is found (see Figs 7, 10, 19 and 20) and a "club-like" morphology is frequently observed (as in Figs 7 and 11). It is possible that this latter morphology develops to equilibrate surface tension forces at the pro-eutectoid ferrite/pearlitic ferrite/cementite triple junction [1, 5]. Continued coarsening will lead to impingement of the individual clubs to form a continuous film at the pearlite/ferrite interfaces. Examples of the coalescence of precipitates at pearlite/ferrite interfaces are given in Figs 26 and 30. In common with the grain boundary films, the source of carbon in the early stages of film formation is likely to be from supersaturated ferrite. Subsequent thickening is most likely controlled by a coarsening reaction. Film formation by the development of cementite on a ferrite/austenite interface prior to impingement with a pearlite colony is likely to be an infrequent occurrence as this mode of film formation would involve the generation of a "ferrite gap" between the film and the cementite lamellae within the pearlite colony [1]. However, reference to Figs 11, 13, 21 and 22 reveals no evidence for a ferrite gap and the pearlitic cementite is continuous with the cementite film.

4.5. The pearlite reaction

The pearlite reaction has been shown to be erratic in nature; certain regions of the specimen were fully transformed to ferrite and pearlite, whilst other regions contained ferrite and austenite only. In addition, in any given region, untransformed pools of austenite coexisted with fully transformed pearlitic colonies (see Fig. 3). The erratic nature of the pearlite reaction is most probably due to a "nucleation limitation", i.e., the rate-controlling process of the pearlite reaction in these steels is nucleation of cementite [5].

Before discussing specific features of the pearlite reaction, it is worthwhile noting that the micrographs presented in Section 3 are two-dimensional images of a three-dimensional feature (e.g. a pearlite colony). However, due to the fact that the pools of austenite and the pearlite colonies formed from them are relatively small, it can be assumed that in the discussion of the initiating mechanism (Section 4.5.2), the initiation site will not be far removed from the plane of polish.

4.5.1. The active nucleus for pearlite

The active nucleus for pearlite has been defined previously [1, 2] and the results of this investigation are in complete agreement with those earlier investigations. Thus the active nucleus for pearlite in hypo-eutectoid steels is pro-eutectoid ferrite since continuity between pro-eutectoid and pearlitic ferrite was almost ubiquitous (see Figs 10, 15, 17 and 18).

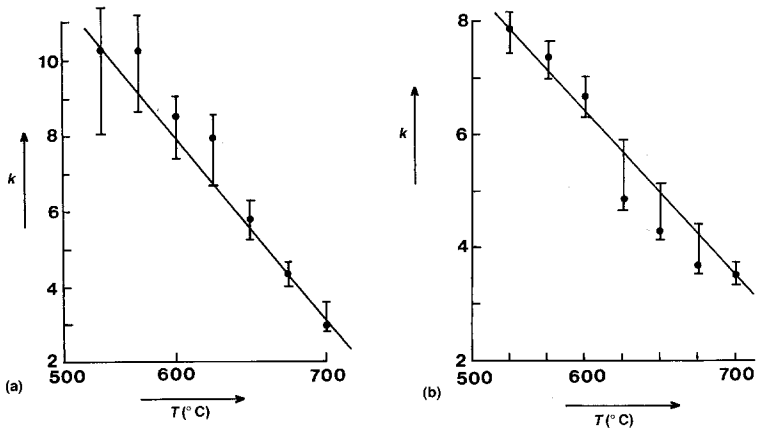

Figure 33 The average aspect ratio of austenite (a) and the average aspect ratio of pearlite (b) as a function of temperature.

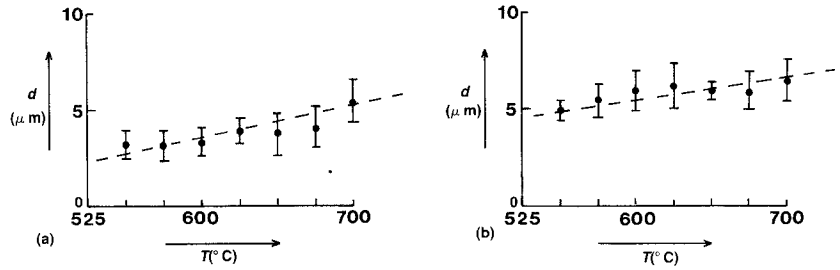

Figure 34 The average size of austenite (a) and the average size of pearlite (b) as a function of temperature.

However, it would appear that only a small fraction of the ferrite/austenite interfaces are effective nucleation sites for the pearlite reaction. This is particularly evident in Figs 19 and 20. For example, in Fig. 20, ferrite grain 1 has initiated the pearlite reaction but no initiation is observed from ferrite grains 2 and 3. The planar nature of the ferrite/austenite interfaces for ferrite grains 2 and 3 suggest that they are of low energy and are not favourable sites for the initiation of the pearlite reaction (nucleation of cementite). This is in agreement with the work of Hillert [2], who suggested that the pearlite reaction could not be initiated when the austenite and ferrite were rationally related. Evidence for the development of partially coherent austenite/ferrite interfaces is given in Fig. 1 where the majority of the ferrite/austenite interfaces are faceted, and secondary side-plates are observed.

4.5.2. Initiation of the pearlite reaction

The model of Hillert [2] is generally accepted for pearlite initiation and involves the formation of a *single* duplex ferrite/cementite nucleus. The pearlite colony is then formed by branching of this single duplex precipitate. In the steels investigated here, one partner (i.e., ferrite) is already present such that the only nucleation event required would be that of a single plate of cementite.

Two consequences of Hillert's model are:

(1) the pearlite colony *must* be divergent in nature and examples of such colonies have been presented by Lee and Howell [1] and Thompson [5];

(2) cooperation between the phases, i.e., the development of the lamellar aggregate, would not be achieved immediately and the initial stage of the reaction will be characterized by a "degenerate" ferrite/carbide aggregate.

In the present investigation, no evidence for the development of a pearlite colony from a single duplex nucleus has been obtained. In addition, no divergent pearlite has been observed.

Cooperation between the phases is seen to be achieved almost immediately and reference to Figs 10, 17 and 18 shows that the lamellar aggregate is present *at* the initiation stage. This is *very* strong evidence that, for the present alloys, *multiple nucleation* of cementite at the austenite/ferrite interface is the formative step in pearlite initiation. Further evidence for multiple nucleation of cementite is provided by the observation of inverse-branching (see Figs 17 and 18). For these colonies more cementite nuclei were present at the initiation interface than were present at the pearlite/austenite interface. This implies that more cementite nuclei can form, than can be sustained during subsequent growth. The images shown in Figs 10 and 15 are also consistent with multiple nucleation but cannot be explained in terms of a single duplex nucleus.

The remaining question then concerns the exact details of the initiating mechanism(s). The most likely mechanisms are similar to those which have been proposed for the development of phenomenologically similar discontinuous reactions given by Fournelle and Clarke [3], Baumann *et al.* [4], Tu and Turnbull [6], and Nes and Billdal [7].

The models of Tu and Turnbull [6] and Baumann *et al.* [4], are similar mechanistically and involve puckering of the grain boundaries. It is tempting to apply these models to the present situation, which would involve nucleation of cementite on the austenite/ferrite interface accompanied by puckering, since

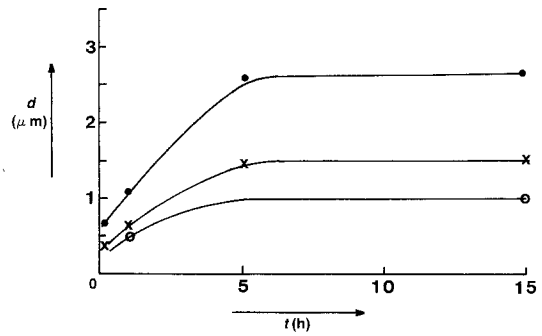

Figure 35 The average cementite film thickness as a function of time. (○) 650° C, (×) 675° C, (●) 700° C.

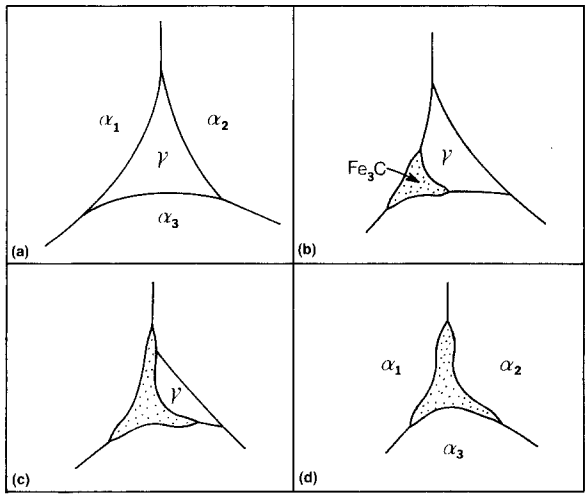

Figure 36 A schematic illustration of the development of cementite films at "ferrite triple junctions". For clarity, the volume fraction of the austenite pool which transforms to cementite has been exaggerated.

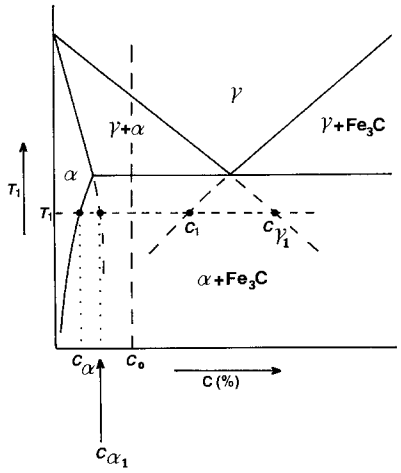

Figure 37 A schematic drawing of the Fe-rich end of the Fe–C phase diagram.

puckering of the ferrite grain boundaries by multiple precipitates of cementite was a frequent occurrence (Section 4.3). However, application of the multiple nucleus model of Baumann *et al.* [4] would suggest that the pearlitic lamellae should be at a relatively low angle to the initiation interface. However, in the vast majority of cases, the pearlite lamellae formed at a high angle to the initiation interface (see Figs 17 and 18). Hence, the dominant initiation mechanism may well be similar to that due to Fournelle and Clarke [3], a model which was developed specifically for initiation on a mobile boundary. This model involves multiple nucleation events followed by branching and re-nucleation which establishes the correct lamellar spacing. The image shown in Fig. 31 bears many similarities with Fig. 9 of Fournelle and Clarke [3].

5. Conclusions

(1) Massive films of cementite on ferrite grain boundaries form from entrapped regions of austenite with a high aspect ratio, or from small volumes of austenite at pro-eutectoid ferrite "triple junctions".

(2) Small discrete precipitates of cementite on the ferrite grain boundaries form from supersaturated ferrite.

(3) Massive films of cementite on ferrite/pearlite interfaces form predominantly by a coarsening mechanism.

(4) Only a fraction of the ferrite/austenite interfaces are effective sites for the nucleation of pearlite. It is suggested that certain ferrite/austenite orientations inhibit the development of pearlite.

(5) No evidence for a branching mechanism for pearlite initiation has been obtained.

(6) The results indicate strongly that multiple nucleation of cementite is the formative step in the initiation of the pearlite colonies in these low carbon steels.

(7) The most probable pearlite initiation mechanism is similar to that developed by Fournelle and Clarke [3] for the phenomenologically similar discontinuous reaction.

Acknowledgements

The authors wish to acknowledge the American Iron and Steel Institute (AISI) and the Atlantic Richfield Foundation for financial support. The authors are also grateful to Dr G. Ludkovsky of Inland Steel, Chicago, for the supply of materials.

References

1. J-W. LEE and P. R. HOWELL, *J. Mater. Sci.* **22** (1987) 3631.
2. M. HILLERT, in "Decomposition of Austenite by Diffusional Processes", edited by V. F. Zackay and H. I. Aaronson (Interscience Publishers, New York, 1962) p. 289.
3. R. A. FOURNELLE and J. B. CLARKE, *Met. Trans.* **3** (1972) 2757.
4. S. F. BAUMANN, J. R. MICHAEL and D. B. WILLIAMS, *Acta Metall.* **29** (1981) 1343.
5. S. W. THOMPSON, PhD thesis, The Pennsylvania State University, University Park, PA 16802, USA (1986).
6. K. N. TU and D. TURNBULL, in "The Mechanisms of Phase Transformations in Crystalline Solids" (Institute of Metals, London, 1969) p. 32.
7. E. NES and H. BILLDAL, *Acta Metall.* **25** (1977) 1039.

Received 3 October 1988
and accepted 27 February 1989